

RADIATION EFFECTS IN SILICON DETECTORS FOR FUTURE HIGH ENERGY PHYSICS EXPERIMENTS: A SHORT OVERVIEW

MARA BRUZZI

I.N.F.N. Firenze – Dipartimento di Energetica di Firenze, Via S.Marta 3, 50139 Firenze, Italy

E-mail: bruzzi@fi.infn.it

Radiation effects in silicon detectors to be used in future high energy physics experiments are discussed. A short overview is given of the major changes in the operational parameters due to radiation damage, and their origin in the radiation-induced microscopic disorder in the silicon bulk. The relevant radiation hardening technologies are described, that have been adopted by the high energy physics community to face the hostile radiation environment where silicon pixel and microstrip detectors will operate in the Large Hadron Collider.

1 Introduction

Silicon-based devices have found since many years application in a wide variety of hostile radiation environments. For this reason, radiation effects in silicon have received extensive attention in the past in order to assess the radiation-induced performance degradation of Si devices. During the last ten years, the increased use of silicon detectors in high energy physics experiments has given a further impulse to this research activity, in an attempt to face the extremely severe radiation environment where silicon devices will operate. This applies in particular to instrumentation at the Large Hadron Collider (LHC) at CERN, providing p-p collisions with a centre of mass energy of 14TeV and an unprecedented luminosity of up to $10^{34} \text{ cm}^{-2}\text{s}^{-1}$ [1,2]. CMS (Compact Muon Solenoid) [3] and ATLAS (A Toroidal Lhc ApparatuS) [4] experiments at LHC are designed to have a highly advanced central tracking detector around the collision region, where high spatial precision and time resolution will be achieved using pixel and microstrip silicon detectors with a total active area of the order of 230m^2 (CMS) and 70m^2 (ATLAS). During the 10 years-lifetime of LHC running this area will be exposed to high energy particle (p, n, π , e) fluences up to 10^{14} cm^{-2} for microstrips and 10^{15} cm^{-2} for pixels [5]. The survival of the silicon detectors placed in the inner tracker region of CMS and ATLAS appears therefore as a major experimental constraint, and has motivated in recent years dedicated radiation-damage research programs carried out by the high energy physics (HEP) community [6]. In this paper, a brief overview of the most important features of radiation damage in silicon detectors is presented.

2 Silicon Microstrip Detectors

Silicon microstrip HEP detectors are usually produced from n-type high resistivity (1-6 k Ω cm) phosphorous doped float zone (FZ) material. Strips are p⁺ boron implants, and the signals from the collected charge is AC coupled to the read-out electronics through integrated capacitors made with thin layers of dielectric. Biasing is accomplished from a p⁺ implant surrounding the active area acting as a bias ring through an array of polysilicon resistors. Typical linear dimensions are: detector thickness $d \approx 300\mu\text{m}$, a single-module length of $\approx 10\text{cm}$, strip width $w \approx 15\mu\text{m}$ and interstrip pitch $p \approx 50\text{-}200\mu\text{m}$. An n⁺ phosphorous layer is implanted on the backside to ensure the ohmic contact, provided by a uniform Al layer. Radiation-damage studies have been carried out in order to investigate the radiation effects in silicon microstrip devices after irradiation simulating 10 years of LHC operation. Tests have been mainly focussed on the radiation-induced defect creation, as well as on the change in the full depletion voltage V_{dep} , e.g. the reverse voltage required to maximize the detector active volume, the effective doping concentration N_{eff} (the net concentration of fixed charge in the depleted layer), the bulk resistivity, the leakage current I_{dep} , the charge collection efficiency CCE and the capacitance contribution to the noise.

3 Microscopic Damage

The study of radiation-induced defects in silicon left a very deep track in literature from the 50's [7] to nowadays. This is due to the continuous improvement of experimental and theoretical capabilities allowing to constantly advance the physical understanding on this subject. A strong improvement in the study of radiation-induced defects came from the 70s thanks to thermal spectroscopic techniques as thermally stimulated currents (TSC) [8], deep level transient spectroscopy (DLTS) [9], photo induced current spectroscopy (PICTS) [10], allowing to determine the activation energy E_t , electron/hole capture cross sections $\sigma_{n,p}$ and concentration N_t of deep defects. A data collection of the most important deep defects observed in silicon is given in [11]. Energy levels lying in the range 0.17-0.40eV are related to defects as vacancy-oxygen (V-O) and divacancy V_2 in different charge states (mainly acceptor-like defects) and carbon-related traps as C_1 , C_1C_s and C_1O_i (donor-like defect). The at least partial removal of the shallow levels related to phosphorous is also induced in silicon by radiation [12], through the creation of phosphorous-vacancy (P-V) complexes introducing an acceptor-like level at about $E_C-0.44\text{eV}$. Midgap defects, characterized by energy levels at $\approx 0.5\text{eV}$ from the valence or conduction band edges, become dominant in the high fluence range, which are believed to be associated to the V_2O , V_3 defects or more generally to extended defects as clusters of divacancies and interstitials. In fact, it is well

known that extended disordered regions are created by irradiation with high energy heavy particles [13].

In the HEP community, since 1995 the RD48 CERN collaboration has adopted the strategy to add selected impurities, in particular oxygen, in the silicon bulk in order to affect the microscopic damage induced by radiation [6]. Oxygen is believed to increase the Si radiation hardness through the capture of radiation-generated vacancies and the production of the V-O complex. In this way O_i acts as a sink of vacancies, thus reducing the probability of formation of the divacancy-related complexes which are responsible for deeper levels inside the gap. In high purity FZ Si, $[O_i] \approx 10^{15} \text{cm}^{-3}$, while in Czochralski (Cz) Si $[O_i] \approx 10^{17}-10^{18} \text{cm}^{-3}$. As the Cz silicon is not available in detector grade quality, a proper oxygenation technique was developed at BNL (Brookhaven National Laboratory) to produce diffusion oxygenated FZ (DOFZ) silicon [14]. The role of oxygen for increasing the silicon radiation hardness was the subject of intensive studies in the old past. In the case of Co^{60} γ -photons irradiation, significant radiation hardening effects were found in 1964 by increasing the oxygen concentration in Si [15]. Conversely, neutron-induced degradation of n-type Si was observed to be independent of the oxygen concentration in 1966 [16]. In fact, in γ -irradiated Si the lattice damage is mainly due to point defects which are interacting with the native impurities, while in neutron-irradiated Si, where the main lattice damage is related to defect clusters, defect-impurity complexes involving O_i are not playing a significant role.

4 Macroscopic Damage

4.1 N_{eff} and bulk resistivity

Fig.1 shows the typical dependence of V_{dep} versus the fluence after a room temperature irradiation with 1MeV neutrons. The data refer to three sets of detectors made with standard n-type FZ Si with different starting resistivity. The change in depletion voltage is related to the change in the effective doping concentration in the space charge N_{eff} , defined by:

$$N_{eff} = \frac{2 \varepsilon V_{dep}}{qd^2} \quad (1)$$

with q electronic charge and ε dielectric constant. An exponential decrease of V_{dep} and consequently of N_{eff} with the fluence f is observed in the low fluence range, a behavior which can be explained in terms of a shallow donor removal process. For higher fluences a linear increase of V_{dep} with f is observed, due to the radiation-induced generation of an acceptor-like state bringing a negative contribution to N_{eff} and leading, for sufficiently high fluences, to the inversion of the sign of the space charge [17].

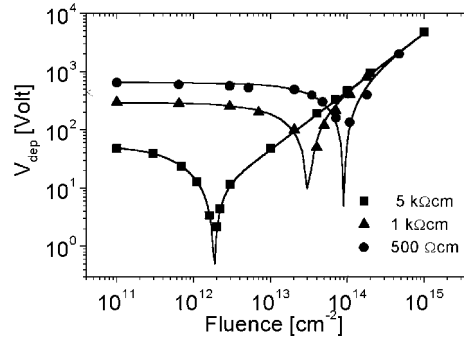


Figure 1. Full depletion voltage measured by CV analysis for three sets of silicon detectors of different starting resistivity after irradiation with 1MeV neutrons.

The fluence at which a minimum in N_{eff} occurs is called *inversion fluence*. One way to shift the inversion fluence towards the high range is the lowering of the starting resistivity. Very low resistivity values are nevertheless not convenient as they will mean very high full depletion voltages: a best compromise is $\rho \approx 1\text{k}\Omega\text{cm}$. In the very high fluence range ($f > 10^{14}\text{ cm}^{-2}$) estimated values of V_{dep} are 10^3 - 10^4V so that it becomes practically impossible to fully deplete the irradiated diode. After irradiation N_{eff} is a function of temperature and duration of the storage: this annealing phenomenon is discussed in detail in [18]. The modification of N_{eff} after irradiation can be described as the combination of different mechanisms. A significant contribution to N_{eff} which makes it increasing with time at room temperature after the inversion fluence, comes from the *reverse annealing* process. To minimize the effect of reverse annealing, the silicon detector should be kept at low temperature during operation, typically -10°C . Under saturation conditions in low compensated silicon $N_{eff} \sim |N_{do}e^{-cf} - \beta f|$ with $\beta = 6.65 \times 10^{-2}\text{ cm}^{-1}$ [18] for standard material. Of note is the fact that, in the case of DOFZ Si irradiated with 24GeV/c protons, β resulted a factor ≈ 3 lower than for standard Si [19].

In irradiated silicon, for fluences high enough to produce inversion, the bulk resistivity (at room temperature) achieves a value close to $100\text{K}\Omega\text{cm}$ independently of the starting doping [20]. A change in sign of the Hall Coefficient from negative to positive, clearly indicating an inversion of the conductivity from n- to p-type, is observed in heavily irradiated high resistivity n-type Si. In the high fluence range, the Fermi level is pinned at $\approx E_v + 0.5\text{eV}$ independently of the starting resistivity and material used (FZ or Cz).

4.2 Leakage current

The leakage current per unit volume measured at full depletion is directly proportional to the fluence f through the constant $\alpha = (3.99 \pm 0.03)10^{-17}\text{ A/cm}$

(determined at 20°C after a thermal treatment of 80min at 60°C) [21] which is independent of the starting resistivity and silicon material. A *beneficial annealing* effect is observed after irradiation as the leakage current is seen to decrease during isothermal annealing at 60°C. The leakage current dependence on T is typically generational: $I_{\text{dep}} \propto T^2 \cdot \exp(-E/kT)$ with $E \sim 0.6\text{eV}$. Test-diodes with active area of 1cm^2 and thickness of $300\mu\text{m}$ achieve room temperature leakage currents up to the order of mA after irradiation with $f \approx 10^{14}\text{cm}^{-2}$. To correctly operate the device after such irradiation, it is necessary to keep the detector at least at -10°C to reduce the leakage current of a factor ≈ 20 .

4.3 Electric field distribution in heavily irradiated Si

Silicon detectors irradiated beyond the inversion fluence can be regarded as a slightly p-type quasi-intrinsic (π) material interfaced with two p^+ and n^+ layers respectively at the front and rear contact sides. To investigate the electric field distribution in such a structure Transient Current Technique TCT [22] was used. A red light laser ($\lambda = 720\text{-}830\text{nm}$ and pulse duration $\approx 1\text{ns}$) illuminates the Si detector: the light penetration is of the order of few microns and laser induced current-pulse shapes are measured to study time-resolved hole and electron transport. It was shown in [23] that, for fluences beyond inversion, an irradiated Si detector is sensitive on both sides for $V_{\text{rev}} < V_{\text{dep}}$ and that a field maximum is observed not only on the rear n^+ contact (as expected from type inversion), but also on the front p^+ contact. The irradiated detector is characterized by a double junction structure: one still placed at the p^+ contact, with $N_{\text{eff}} > 0$, and a second at the n^+ contact, characterized by $N_{\text{eff}} < 0$. A sketch of the band bending at equilibrium in the heavily irradiated detector is shown in fig. 2.

The two space charge regions originate from the ionization of the deep levels near midgap, mainly due to clusters, divacancy related defects and C_iO_i . In this picture, donor-like defects are mostly distributed in the lower half of the forbidden gap, while acceptor-like states are lying in the upper half. An estimation of the electric

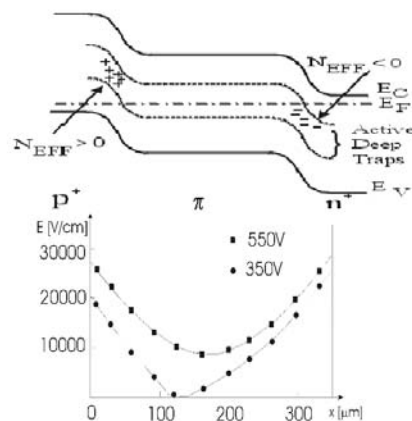


Figure 2. Sketch of the energy band bending in an irradiated pad silicon detector at $V_{rev} = 0$ and (bottom) calculated electric field profile in a heavily irradiated silicon in full- and over-depletion conditions.

field distribution in a silicon detector irradiated beyond 10^{14} cm^{-2} is given in the bottom of fig. 2 for $V_{rev}=350\text{V}$ (depletion voltage) and 550V . The curves, redrawn from [24], have been determined using a model where two deep levels, with activation energy at 0.52eV respectively above the valence band edge and below the conduction band edge, are supposed to be responsible of the double junction. The depletion region is splitted into two parts which at sufficiently high bias join together (pinch-off effect).

4.4 Charge Collection Efficiency

In non-irradiated devices the CCE is directly proportional to the depletion depth and consequently to the square root of the applied voltage V_{rev} and saturates to 100% at full depletion. When operated at room temperature, the silicon detectors suffer a drastic decrease in the charge collection efficiency for fluences higher than 10^{14} cm^{-2} [25]. A model to describe the charge collection efficiency in irradiated silicon detectors is given in [26]. For a fast shaping read-out as needed for the LHC (25ns) a significant amplitude reduction in the CCE is observed (“ballistic deficit”) in heavily irradiated, partially depleted detectors: the reduction factor is dependent on the reverse voltage, as it is given by the ratio between the depletion depth and the total thickness: W/d . At full depletion, this factor is no more significant, and the trapping of free carriers is the main cause of charge collection reduction, as discussed in [27]. To allow the total depletion after hadron irradiation over 10^{14} cm^{-2} it is necessary to operate the device at low temperature: typically -10°C . As the leakage current strongly contributes to fill the deep traps which are responsible for the high N_{eff} observed in heavily irradiated silicon, keeping the detectors in a cold

environment significantly reduces also the bias required to maximize the CCE [24]. This is the reason why the CCE signal of an heavily irradiated detector is observed to significantly rise at low temperatures (“*Lazarus Effect*”) [27].

If the CCE vs. V_{rev} curve is compared with the C-V characteristic of a heavily irradiated detector, one observes that the depletion voltage obtained from C-V corresponds to a CCE value which is approximately 75-80% its maximum value. To achieve a 95-100% charge collection it is necessary to apply a voltage which is almost twice V_{dep} [28,29,30]. ATLAS microstrip detectors with p-strip read-out made with DOFZ Si, irradiated up to $3 \times 10^{14} \text{ cm}^{-2}$ with 24 GeV/c protons have been tested to study this effect. The results do not show a major advantage in using DOFZ Si in terms of the required operating voltage to maximise the CCE. The slope of the CCE vs. V_{rev} curve is higher for the oxygenated material, but above the full depletion voltage obtained by C-V, the CCE continues to rise significantly with bias. The voltage required to obtain a 95% charge collection efficiency with oxygenated Si after this study is only $\sim 50\text{V}$ lower than in standard material. This effect could be related to the peculiar shape of the electric field distribution, characterized by a minimum in the central bulk of the detector. This minimum should be increased over some critical value by further increasing the bias over the full depletion voltage to maximize the charge collection efficiency from the entire detector volume. Of note is the fact that, with the n^+ -strip detector read-out technology firstly developed by ATLAS, the charge collection efficiency maximum was actually achieved at full depletion [28]. This suggests that the double peaked electric field distribution should be asymmetrical in shape, allowing a better efficiency in collecting charge through the n^+ side as compared to the p^+ side.

4.5 Capacitance contribution to the noise

Irradiated silicon microstrip detectors have been tested to study the signal to noise ratio S/N under the LHC read-out electronic conditions. In deconvoluted mode ($\tau=25\text{ns}$), the noise contribution due to the total input capacitance in CMS is estimated to be $ENC \sim 1000e^- + 46e^-/\text{pF}$. Recently, studies performed in the framework of the CMS collaboration evidenced a significant contribution to the noise after irradiation due to the increase in the interstrip and backplane capacitances in the case Si $\langle 111 \rangle$ crystal is used. In microstrip detectors a large part of the surface is covered by oxide, which can lead to a significant radiation-induced surface damage, related to interface traps and oxide charges located at the Si-SiO₂ system. Close to midgap the interface trap density is almost one order of magnitude higher for $\langle 111 \rangle$ crystal orientation than for $\langle 100 \rangle$, due to the higher number of available dangling bonds at the crystal surface in $\langle 111 \rangle$. As a result, inter strip and back plane capacitances (C_{int} , C_{back}) of microstrip detectors manufactured using $\langle 100 \rangle$ Si are less affected by radiation than those produced from $\langle 111 \rangle$ oriented Si [31]. This effect is observed on the p-side of inverted detectors for bias voltages

below full depletion, whereas comparable C_{int} and C_{back} values are measured when $\langle 100 \rangle$ and $\langle 111 \rangle$ Si-based devices are operated in over-depletion conditions.

5 Conclusions

The large scale application of silicon microstrip and pixel detectors to provide precision tracking of charged particles at the future CERN Large Hadron Collider (LHC) experiments has triggered in recent years an extensive research activity focussed on the radiation-induced degradation of such devices in the anticipated environment. The main aspects and results of this work have been discussed in this paper. The requirements for the silicon detectors are a single-strip binary readout threshold of 1fC for ATLAS and a signal-to-noise ratio $S/N \approx 10$ in de-convolution mode for CMS. Measurements performed on silicon microstrip detectors irradiated up to 1MeV neutron fluences of 10^{14} cm^{-2} , corresponding to approximately ten years operation of LHC, proved that silicon detectors can match these performances provided that certain technological improvements are implemented. An efficient cooling system must be installed to keep the overall silicon active area at temperatures around -10C during operation and, possibly, during almost all the beam-off period. Radiation-hardening technologies have been proposed and are presently under study to control the performance degradation through the introduction of selected impurities in the silicon bulk. A significant lowering of the full depletion voltage V_{dep} derived by C-V measurements after γ and proton irradiation has been observed when oxygen enriched FZ silicon is used. Surface damage reduction is observed by using $\langle 100 \rangle$ oriented Silicon. However, as over-depletion is required to maximize the charge collection efficiency, the operational advantages of using oxygenated devices and $\langle 100 \rangle$ orientation are significantly reduced. More studies are in progress to understand these effects in more depth and to further improve the radiation hardness of silicon microstrip and pixel detectors.

References

1. The Large Hadron Collider, conceptual design, The LHC study group, CERN/AC/95-05 (LHC), 20 October 1995.
2. J.Varela, "Physics at the Large Hadron Collider," *Nucl. Physics B* **37C** (1995) pp.121-134.
3. "The Compact Muon Solenoid, Technical Proposal," CERN/LHCC 94-38 LHCC/P1, 1994.
4. ATLAS Technical Proposal, CERN/LHCC/94-43, LHCC/P2,1994.
5. Pertti A. A. Arnio, Mika Huhtinen, "Hadron fluxes in the inner parts of LHC detectors, *Nucl. Instrum. Meth. A* **336** (1993) pp. 98-105.

6. G.Lindström et al. "Radiation Hard Silicon Detectors-Developments by the RD48 (ROSE) Collaboration," *Nucl. Instr. Meth. A*.
7. Radiation Effects in Semiconductors, May 6-9, 1959, Gatlinburg, Tennessee, *J. Appl. Phys.*, **30**, n.3, (1959).
8. M. G. Buehler, Impurity centers in *pn* junctions determined from shifts in the thermally stimulated current and capacitance response with heating rate, *Solid-State Electronics* **15** (1972) pp. 69-79.
9. D.V. Lang, Deep-level transient spectroscopy: a new method to characterize traps in semiconductors, *J. Appl. Phys.* **45** (1974) pp. 3023-3032.
10. A.Blood and J.W.Orton, "The electrical characterization of semiconductor: majority carriers and electron states," N.H.March, *Ed. Academic Press*, London, 1992.
11. Mara Bruzzi, Radiation damage in silicon detectors for high-energy physics experiments, *IEEE Trans.Nucl. Sci.* **48** (2001) pp.960 –971.
12. E.Borchi, M.Bruzzi, Z.Li, S.Pirollo, Thermally Stimulated Currents Analysis of the Shallow Levels in Irradiated Silicon Detectors, *J. Phys. D: App. Phys.* **33** (2000) pp. 299-304.
13. V.A.J. van Lint, T.M.Flanagan, R.E.Leadon, J.A.Naber, V.C.Rogers, "Mechanisms of Radiation Effects in Electronic Materials," John Wiley & Sons, 1980.
14. Z.Li et al., Investigation of the oxygen-vacancy (A-center) Defect complex profile in neutron irradiated high resistivity silicon junction particle detectors, *IEEE Trans. Nucl. Sci.*, **NS-39** (1992) pp. 1730-1738.
15. T.Nakano, Y.Inuishi, Effects of Dosage and Impurities on Radiation Damage of Carrier Lifetime in Silicon, *J. Phys. Soc. Japan* **19**, (1964), pp. 851-858.
16. O.L.Curtis, Jr., "Effects of oxygen and dopant on lifetime in neutron-irradiated silicon," *IEEE Trans. Nucl. Sci.*, **NS-13** (1966) pp. 33-40.
17. E.Borchi and M.Bruzzi, "Radiation Damage in Silicon Detectors," *La Rivista del Nuovo Cimento*, **17** (1994).
18. G.Lindström, M.Moll, E.Fretwurst, "Radiation hardness of silicon detectors – a challenge from high energy physics," *Nucl. Instr. Meth. A* **426** (1999) pp. 1-15.
19. A.Ruzin, G.Casse, M.Glaser, A.Zanet, F.Lemeilleur, S.Watts, "Comparison of radiation damage in silicon induced by proton and neutron irradiation," *IEEE Trans. Nucl. Sci.* **46** (1999) pp. 1310-1313.
20. E.Borchi, M.Bruzzi, B.Dezillie, S.Lazanu, Z.Li, S.Pirollo, "Hall effect analysis in irradiated silicon samples with different resistivities," *IEEE Trans. Nucl. Sci.*, **46** (1999) pp. 834-838.
21. M.Moll, E.Fretwurst, G.Lindström, "Leakage current of hadron irradiated silicon detectors–material dependence," *Nucl. Instr. Meth. A* **426** (1999) pp. 87-93.

22. V.Eremin and Z.Li, "Determination of the Fermi level position for neutron irradiated high resistivity silicon detectors and materials using the transient charge technique (TChT)," *IEEE Trans. Nucl. Sci.* **41** (1994) pp. 1907-1912.
23. Z.Li and H.W.Kraner, "Modeling and simulation of charge collection properties for neutron irradiated silicon detectors," *Nucl. Phys. B* **32** (1993) pp. 398-409.
24. V.Eremin, E.Verbitskaya, Z.Li, Effect of Radiation Induced Deep Level Traps on Si Detector Performance, in press *Nucl. Instr. Meth. A* (2001).
25. E. Borchì, M. Bruzzi, C. Leroy, S. Pirollo, S. Sciortino, Charge collection and noise analysis of heavily irradiated silicon detectors, *IEEE Trans.Nucl. Sci.* **45** (1998) pp.141 –145.
26. V.Eremin, N.Strokan, A.Verbitskaya, Z.Li, "Development of transient current and charge techniques for the measurement of effective net concentration of ionized charges (N_{eff}) in the space charge region of p-n junction detectors," *Nucl. Instr. Meth. A* **372** (1996) pp.388-398.
27. W.H.Bell, L.Casagrande, C.DaVia, V.Granata, V.G.Palmieri, "Temperature dependence of the charge collection efficiency in heavily irradiated silicon detectors," *Nucl. Instr. Meth. A* **435** (1999) pp. 187-193.
28. P.P.Allport, L.Andricek, C.M.Buttar, J.R.Carter, M.J.Costa, L.M. Drage, et al. "A comparison of the performance of irradiated p-in-n and n-in-n silicon microstrip detectors read out with fast binary electronics," *Nucl. Instr. Meth. A* **450** (2000) pp. 297-306.
29. S.Marti i Garcia, P.P.Allport et al., Charge collection efficiency of irradiated p⁺n wedge silicon microstrip detectors for ATLAS, *Nucl. Instr. Meth.A* **426**, (1999) pp. 24-27.
30. A.Buffini, S.Busoni, E.Catacchini, C.Civinini, R.D'Alessandro, E.Focardi, M.Lenzi, M.Meschini, C.Minelli, G.Parrini, Characterization of neutron irradiated silicon microstrip detectors, in press *Nucl. Instr. Meth. A* (2001).
31. G. Calefàto et al., A comparison on radiation tolerance of <100> and <111> silicon substrates of microstrip detectors, in press *Nucl. Instrum. & Meth. A* (2001).